Influence of Sapphire Substrate Orientation on the van der Waals Epitaxy of III-Nitrides on 2D Hexagonal Boron Nitride: Implication for Optoelectronic Devices

Phuong Vuong, Suresh Sundaram, Vishnu Ottapilakkal, Gilles Patriarche, Ludovic Largeau, Ashutosh Srivastava, Adama Mballo, Tarik Moudakir, Simon Gautier, Paul L Voss, et al.

Influence of Sapphire Substrate Orientation on Van der Waals Epitaxy of III-Nitrides on 2D Hexagonal Boron Nitride: Implication for Opto-electronic Devices

Phuong Vuong[1], Suresh Sundaram[1,2], Vishnu Ottapilakkal[1], Gilles Patriarche[3], Ludovic Largeau [3], Ashutosh Srivastava[1,2], Adama Mballo[1], Tarik Moudakir[4], Simon Gautier [4], Paul L. Voss[1,2], Jean-Paul Salvestrini[1,2], and Abdallah Ougazzaden[1,2,]*

[1]Georgia Tech Lorraine, IRL 2958 – CNRS, 57070 Metz, France
[2]School of Electrical and Computer Engineering, Georgia Institute of Technology, Atlanta, GA 30332, USA
[3]Centre de Nanosciences et de Nanotechnologies, Université Paris-Saclay, C2N – Site de Marcoussis, Route de Nozay, F-91460 Marcoussis, France
[4]Institut Lafayette, 2 rue Marconi, 57070 Metz, France

* Correspondence: abdallah.ougazzaden@georgiatech-metz.fr

Abstracts:

Van der Waals (vdW) epitaxy of three-dimensional (3D) device structures on two-dimensional (2D) layers is particularly interesting for III-nitrides because it may relax lattice matching and thermal mismatch requirements and can permit convenient lift-off of epilayers and opto-electronic devices. In this article, we report vdW epitaxy of 3D GaN/AlGaN on 2D h-BN grown on *a*-, *c*-, and *m*-plane sapphire substrates via metal-organic chemical vapor phase epitaxy. First, we study 2D h-BN layers grown on *a*-, *c*-, and *m*-plane sapphire to demonstrate the substrate effect on h-BN growth and h-BN alignment. We find that h-BN can align itself to its preferred *c*-axis with a slight misorientation on *m*-plane sapphire substrate. However, the difference in crystallographic orientation, thermal expansion coefficient, and surface energy of differently oriented sapphire substrates strongly influence the surface morphology (good for *a*- and *c*- plane) and the adhesion of h-BN layers (lift-off only possible for *c*-plane). Second, vdW growth of 3D GaN/AlGaN on 2D h-BN grown on *a*-, *c*-, and *m*- planes of sapphire was investigated. HR-XRD 2θ-ω scan and selected area electron diffraction pattern was used to demonstrate the misorientation of GaN/AlGaN grown on 2D h-BN/*m*-plane sapphire compared to polar GaN grown on 2D h-BN/*a*- and *c*-plane sapphire. It was found that the morphology and crystalline quality of GaN/AlGaN is directly affected by the 2D h-BN layers. These results provide initial insight into the impact of substrate orientation, thereby acting as a guide for potential design of III-nitride/h-BN vdW epitaxy seeking to use non-polar or semi-polar planes of sapphire for opto-electronic devices such as LEDs, high power electronics and detectors.

Keywords: van der Waals epitaxy, Metal-organic chemical vapor phase epitaxy (MOVPE), two-dimensional materials, hexagonal Boron Nitride, III-nitrides, substrate orientations.

Introduction:

Van der Waals (vdW) epitaxy was discovered as early as 1984 [1] and has proven to be a beneficial approach for heteroepitaxy growth [2–6]. Recently, vdW epitaxy of three-dimensional (3D) materials on two-dimensional (2D) layers has attracted tremendous attention. Compared to conventional 3D/3D epitaxy, the bonds between 3D epilayer and 2D buffer layer are about two orders of magnitude weaker [3]. This weak vdW bond can be very advantageous for 3D/2D epitaxy, accommodating thermal and lattice mismatches with substrates, which may dramatically improve the crystalline quality of 3D materials [6–8]. Moreover, thanks to the layered structure of 2D materials, 3D heterostructures can be mechanically detached from their substrate over a large area and transferred as membranes to arbitrary carriers with simple flexible, soft or hard holders (tapes, PDMS, metals) [9,10] .

III-nitride semiconductors are well known as perfect candidates for light-emitting diodes (LEDs), lasers diodes (LDs), high electron mobility transistors (HEMTs) and other opto-electronic devices. VdW epitaxy has been confirmed to be a suitable method for III-nitride epitaxy, which has the potential to enhance the performance of III-nitride devices. Among vdW 2D materials, h-BN is an excellent choice as a buffer layer for the III-nitride vdW epitaxy due to the following reasons: i) chemical stability at III-N growth temperature, ii) the surface is favorable for the nucleation of 3D III-nitride materials iii) the growth conditions are compatible with different industrial deposition systems (MOVPE, MBE, CVD), and iv) the availability of the boron precursors as organometallic gas sources.

In addition, the substrate used in vdW III-Nitride epitaxy also plays an important role because it affects the crystal orientation and the strain of the vdW epilayers. The growth of 2D h-BN and 3D III-Nitride semiconductors has been performed on different types of substrates ranging from metals (Ni , Cu) [11–13] to dielectric surfaces and graphene [14,15]. However, sapphire substrates are standard in industry, and exhibit high hardness, good light transmittance and thermal stability [16,17]. As an anisotropic material, the different crystal orientations have different surface and mechanical properties and thereby, can have an impact on vdW epitaxy. It has been reported that GaN grown directly on *a*- and *m*-plane sapphire substrates is non-polar and semi-polar [18–20], which

leads to better luminescence efficiency of the devices when compared with GaN grown on *c*-plane sapphire, which suffers from the quantum-confined stark effect due to strong piezoelectric fields [21]. However, the epitaxy of III-Nitride heterostructures on non-polar sapphire substrates with a 2D interfacial layer has not been previously reported.

The goal of this work is to study the effect of orientation of sapphire substrate on the growth of 2D h-BN layer and subsequent 3D III-Nitride material epilayers through the h-BN buffer layer. We have first investigated the impact of *a*-, *c*- and *m*-plane oriented sapphire substrates on the growth mechanism and alignment of 20 nm thick h-BN layers. Then, vdW epitaxy of GaN/AlGaN epilayers using 1.5 nm thick h-BN as interfacial layer were grown on *a*-, *c*- and *m*-plane oriented sapphire substrates. The dependence of the crystalline structure orientations, morphology of the 2D h-BN layer and III-N epilayers and their adhesion epilayer with different substrate orientations will be discussed. This study can give us a better understanding of the vdW epitaxy of 3D III-Nitride on 2D h-BN materials, motivating further exploration of III-nitride device structures based on vdW epitaxy for opto-electronic devices such as LEDs, high power electronics and detectors.

Experiments:

The growth was performed in an Aixtron MOVPE Close Coupled Showerhead (CCS) reactor on 3x2 inch sapphire substrates. Triethylboron (TEB), trimethylaluminium (TMAl), trimethylgallium (TMG), and ammonia (NH_3) were used as B, Al, Ga, and N precursors, respectively. Two sets of samples were grown. The first set consists of 20 nm thick h-BN layers grown on 2-inch (*a*-, *c*- and *m*-plane) sapphire substrates at 1280°C, which allows us to investigate the effect of the substrate orientations on the growth of h-BN template. The growth rate of h-BN on different sapphire orientation was estimated by scratch and AFM technique (see supplementary-section 1). The second set consists of 500 nm thick GaN layers, using an intermediate 300 nm thick AlGaN (14% Al) layer, grown on 1.5 nm h-BN layer/sapphire substrates (*a*-, *c*- and *m*-plane). Growth of all three sapphire substrates (*a*-, *c*- and *m*-plane) took place in the same run under identical conditions.

Scanning electron microscope (SEM) and atomic force microscopy (AFM) were used to study the surface morphology of the samples before and after mechanical lift-off. The crystalline structure of the h-BN layer and the GaN/AlGaN/h-BN epilayers grown on differently oriented sapphire substrates was investigated by high-resolution X-ray diffraction (HR-XRD) scans,

performed in a Panalytical X'pert Pro Materials Research Diffractometer system using Cu Kα radiation in triple axis mode. This type of experiment allows us to study the diffraction of crystallographic planes parallel to the surface. It will be referred as out-of-plane diffraction in the following. To identify and confirm the orientation of h-BN ultra-thin layers, non-coplanar grazing-incidence X-ray diffraction (GIXRD) measurement were performed using a Rigaku Smartlab diffractometer equipped with a Cu rotating anode and a 5-circle goniometer. The non-coplanar GIXRD geometry allows us to collect the diffraction of the crystallographic planes normal to the sample surface. This type of experiment will be called in-plane diffraction in the following. High-angle annular dark field scanning transmission electron microscopy (HAADF-STEM) characterizations were performed on an aberration-corrected ThermoFisher Titan 200 keV electron transmission microscopy to investigate the structural characterization at the nanoscale. Prior to this study, cross-sectional lamellae were prepared using focused ion beam (FIB) thinning and ion milling after coating a 100 nm thick carbon for layer protection.

Results and discussions:

We first address characterization of 20 nm h-BN grown on *a*-, *c*-, and *m*-plane sapphire substrates. Figure 1 presents SEM and AFM images of the three set of samples. A wrinkled surface is observed for the three h-BN samples grown on *a*-, *c*- and *m*-plane sapphire substrates with a variation in the size and shape of the wrinkles in each sample. The root mean square (rms) roughness of the h-BN grown on *a*-, *c*- and *m*-plane sapphire substrates are 3.2 nm, 3.7 nm, and 2.7 nm, respectively. As reported earlier [22–24], the formation of wrinkles in h-BN layer surface is an indicator of the high structural quality of the layered h-BN. It results from the thermal expansion coefficient (TEC) difference between h-BN and sapphire substrates, which induces a compressive strain in the layer during the cooling process. The wrinkling instability releases the energy, which creates roughness in the sample. The observation of wrinkles in the samples confirms the growth of h-BN layers on the three different sapphire orientations.

An interesting observation is the difference in wrinkle size and shape of the h-BN layer grown on *a*-, *c*- and *m*-plane sapphire substrates. Wrinkled surface of h-BN grown on *a*- and *c*-plane sapphire exhibited an organized semi-hexagonal shape with an average size of 416 nm and 490 nm, respectively. The larger size of h-BN wrinkles grown on *c*-plane sapphire substrate can be explained by isotropic biaxial compressive strain which originates due to difference in values

of the thermal expansion coefficients (TEC) in the oriented sapphire substrates. The compressive strain [25] can be expressed as follow:

$$\Delta\varepsilon = \int_{RT}^{T_G} \alpha_{h-BN}(T) - \alpha_{sapphire}(T)dT \quad (1)$$

where α_{h-BN} (1.91×10^{-9} T $- 2.96 \times 10^{-6}$) $^{\circ}C^{-1}$) and $\alpha_{sapphire}$ are the linear thermal expansion coefficients of h-BN and the sapphire substrate; T_G and RT are the growth temperature and room temperature, respectively. Since the values of TEC is different for *a*-plane ($\alpha_{a-sapphire}$(T) = (9.5×10^{-9}T + 3.83×10^{-6}) $^{\circ}C^{-1}$) and *c*-plane sapphire ($\alpha_{c-sapphire}$(T) = (13.6×10^{-9}T + 3.46×10^{-6}) $^{\circ}C^{-1}$) [24, 26], using these values in equation (1) results in two different values of compressive strain which are -1.76% and -1.47% respectively. This 0.3% difference in the strain value due to TEC of h-BN grown on *a*- and *c*- plane sapphire has an impact on wrinkle formations, resulting in different size of h-BN wrinkle domains as seen in figure 1a-b &d-e.

In the case of h-BN grown on *m*-plane sapphire, wrinkles are in a different formation and shape compared to the ones grown on *a*- and *c*-plane sapphire. They are aligned along sapphire *a*-axis, together with some line feature parallel to sapphire *m*-axis, which is less pronounced (figure 1c&f). Apart from TEC, another factor that can also affect the formation of wrinkles is the crystallographic difference between oriented sapphire substrates. Although, the *a*-plane and *m*-plane are both parallel to the *c*-axis, they might exhibit different material properties such as surface energy, mechanical property due to their different atomic arrangements. This phenomenon may lead to variation in incorporation probability and diffusion length of surface atoms along different crystallographic directions, subsequently causing wrinkles to be more pronounced along sapphire *a*-axis in case of h-BN grown on *m*-plane sapphire substrate. This result provides the first evidence of the effect of sapphire orientation on h-BN.

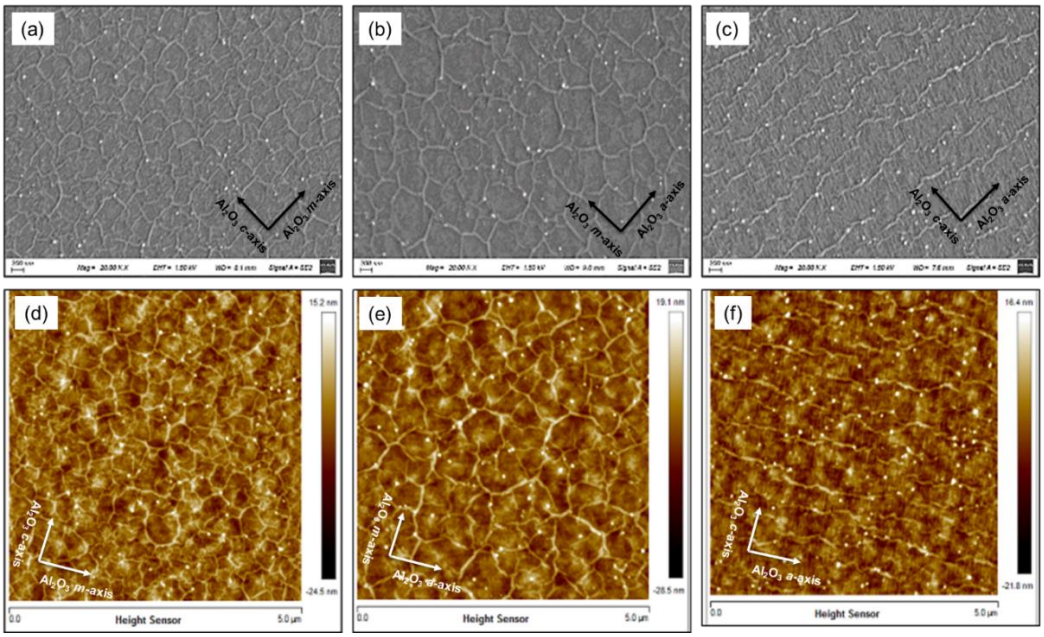

Fig. 1. SEM and AFM images of h-BN grown on a-plane (a&d), c-plane (b&e) and m-plane (c&f) sapphire.

HR-XRD measurements can also provide better understanding on the structural properties and orientation of these set of h-BN layers. Figure 2 shows the out-of-plane 2θ-ω scans of 20 nm h-BN. The prominent diffraction peaks for *a*-, *c*- and *m*-plane sapphire are observed at 37.6°, 41.5°, and 68.7° respectively. The three sets of h-BN layers grown on different plane sapphire substrates exhibit a diffraction peak at around 26.0° and 53.7° which is attributed to h-BN (002) and (004) crystal planes, respectively. It is to be noticed that the (004) plane diffraction peak is very weak for the h-BN layer grown on *a*- and *m*-plane sapphire substrates. The observation of (002) h-BN diffraction peak in these out-of-plane 2θ-ω scans for the three set of samples indicates that the preferred orientation of h-BN is along the *c*-axis (figure 2b). h-BN has strong in-plane sp_2 covalence bonds compared to vdW force between atomic layers. During the growth process, boron and nitrogen atoms may tend to bond to each other inside the layer, resulting in preferable *c*-axis growth direction. This is consistent with the report that under specific thermodynamic conditions, hexagonal materials have tendency to self-align along its natural axis. Miyagawa *et al.* [27] reported that at high growth temperature (1430-1500°C), *c*-plane AlN was obtained when it was grown on *a*-plane sapphire. Shigeya's group also reported that variation of growth temperature of GaN on *r*-plane sapphire led to different oriented GaN (*c*-plane GaN was obtained when grown at low temperature - less than 675°C whereas, *a*-plane GaN was obtained at middle growth temperature

675-690°C) [28]. The same behavior is obtained for 2D h-BN material where its orientation is found to be in a preferred *c*-axis under our growth temperature at 1280°C.

In addition, the low intensity and the higher broadness of the full width at half maximum (FWHM) of (002) h-BN diffraction peak indicates the misorientation of h-BN (or disordered BN) grown on *m*-plane sapphire, where the h-BN layered sheets are confined in short domains and irregularly oriented, losing long range order (figure 2c). The misorientation of h-BN/*m*-plane sapphire and the structural property difference of h-BN grown on *a*-, *c*- and *m*-plane sapphire may be related to the surface energy of different sapphire substrates. Several studies have demonstrated that the surface energy of substrates have a pronounced impact on the crystallographic orientation [2,29,30]. It has been shown that SnO film orientation is related to surface energy of growth substrates [29]. Qi Chen *et al.* [2] also reported that high surface energy or low migration barrier of substrates may induce misorientation or the 3D island growth mode for epitaxial layers. Surface free energy of sapphire with various orientations have been studied theoretically and experimentally [31,32]. It was reported that the surface energy of *c*-plane sapphire (3.357 J/m^2) < *a*-plane sapphire (3.858 J/m^2) < *m*-plane sapphire (7.126 J/m^2) [32]. The high surface energy of *m*-plane sapphire compared to *a*- and *c*-plane sapphire may explain the misorientation of h-BN grown on *m*-plane sapphire.

To identify and confirm the orientation of h-BN ultra-thin layers, we have performed in-plane non-coplanar GIXRD diffraction on the three set of h-BN samples grown on *a*-, *c*- and *m*-plane sapphire as seen in figure 2d-f. The schematic of the experiments is shown in the inset of figure 2d. For *a*- and *c*-plane sapphire samples, the figure 2d&e shows $2\theta\chi/\varphi$ scans collected along the in-plane <100> Al_2O_3 azimuthal direction. Since no monochromator has been used for these measurements, substrate Cu-Kβ and W-Lα diffraction peaks are observed as displayed in figure 2d-f. We have identified two peaks at 41.62° and 75.98°, which may be attributed to (100) BN and (110) BN. The observation of both (100) BN and (110) BN peaks in the same $2\theta\chi/\varphi$ scan indicates that within the whole volume probed by the X-Rays, there are some crystalline parts with in-plane <100> direction parallel to the <100> Al_2O_3 direction and others with <110> direction parallel to the <100> Al_2O_3 direction. It suggests that the h-BN layer is made of grains c-textured but with different in-plane orientations. To confirm this point, a 360° φ scan has been performed for h-BN grown on *c*-plane sapphire (see supplementary-section 2). For h-BN grown on *m*-plane sapphire, the figure 2f shows $2\theta\chi/\varphi$ scans collected along the in-plane <001> Al_2O_3 azimuthal direction. A

diffraction peak at 76.6° was observed and attributed to (110) BN. It reveals that (110) BN is aligned with the (001) Al_2O_3. These observations of (100) BN and (110) BN parallel to (100) Al_2O_3 for *a*- and *c*-plane sapphire, and (110) BN parallel to (001) Al_2O_3 for *m*-plane sapphire confirm that the h-BN growth direction is *c*-axis in these three cases. In addition, we also observe a peak at 33.45° in figure 2d, which may correspond to (100) AlN. It can be related to the presence of AlN underneath h-BN layer due to nitridation, which will be discussed later.

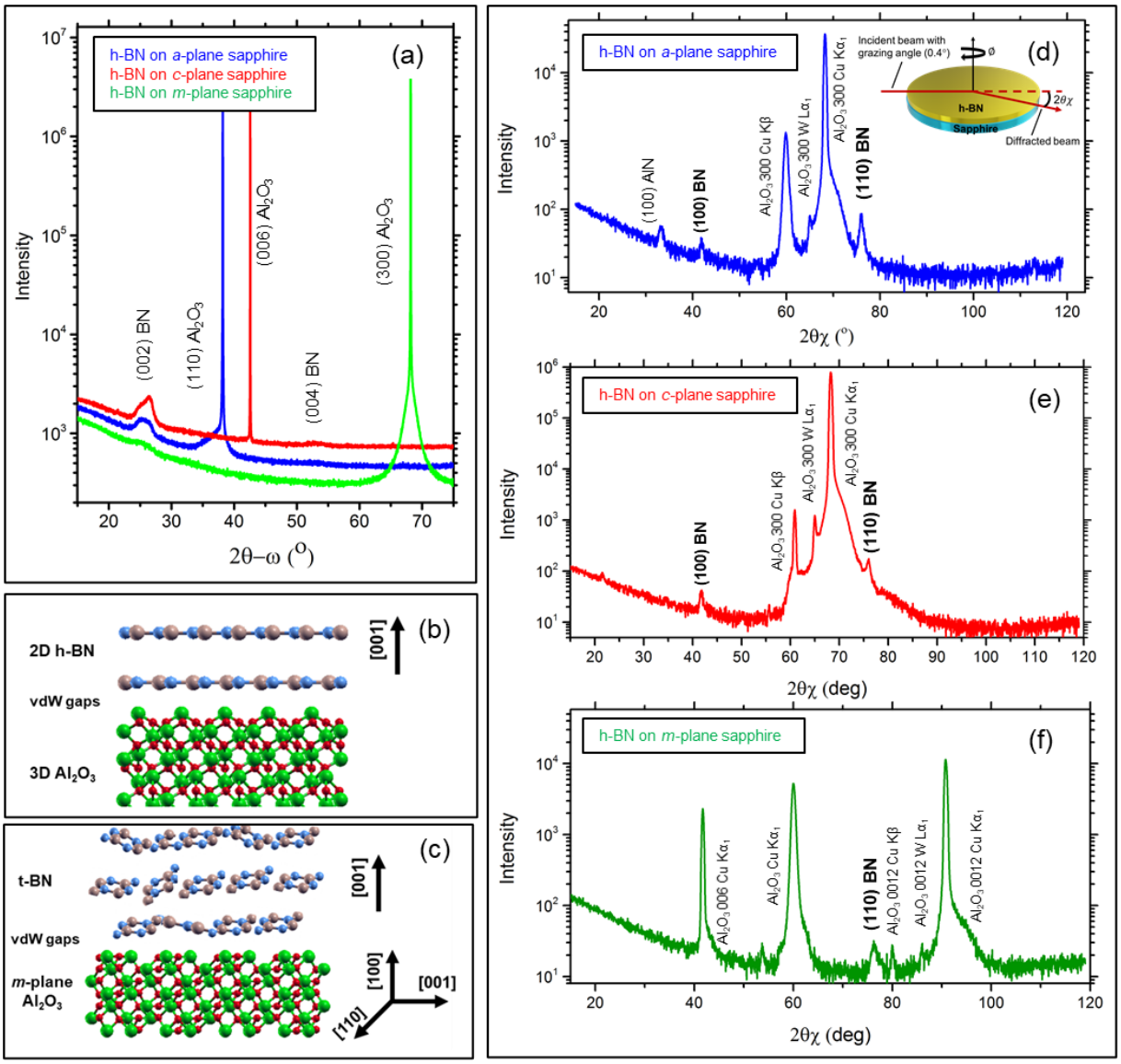

Fig. 2. (a) HR-XRD 2θ-ω scan; b-c) schematic of preferred orientation of h-BN grown on different sapphire orientation; (d-f) GIXRD of 20 nm h-BN on a-, c- and m-plane sapphire. Inset of figure 2d: The schematic of the GIXRD experiments.

To investigate the impact of orientation of sapphire substrates on the control of the mechanical adhesion of h-BN, mechanical lift-off of 20 nm h-BN grown on *a*-, *c*-, and *m*-plane sapphire was studied. Corresponding optical and AFM images are presented in figures 3a-d. For h-BN grown on *c*-plane sapphire the mechanical lift-off occurred using simple scotch tape (figure 3b), which is in agreement with our previous study [33]. Figure 3e shows the corresponding profile as extracted from the AFM image (figure 3d). A thickness difference between the lifted-off region and non-lifted-off region was measured to be around 18 ± 2 nm. However, for *a*- and *m*-planes sapphire, the lift-off of h-BN was not possible despite several attempts (figure 3a&c). It is an interesting result, which has never been reported and shows that the vdWs h-BN layer cannot be mechanically detached in all type of substrate orientations by using soft holder like scotch tape in our case. A possible interpretation of this could be linked to the structural quality (i.e.: the ordered layered lattice) of h-BN layer as reported by Sundaram *et al.* [34]. The misorientation of h-BN grown on *m*-plane sapphire may hinder complete lift-off of the grown layer. Another possible explanation for this might be related to a surface energy of sapphire substrates. The *a*- and *m*-plane sapphires have higher surface energy (as mentioned above) that can enhance the mechanical adhesion between substrate and h-BN, thereby impacting the possibility of lift-off of this layer. We believe that the mechanical lift-off of h-BN grown on *a*-, *c*- and *m*-plane substrates depends on several factors such as structural quality of h-BN and/or surface energy of sapphire substrates. For more quantitative interpretation, further investigations are needed.

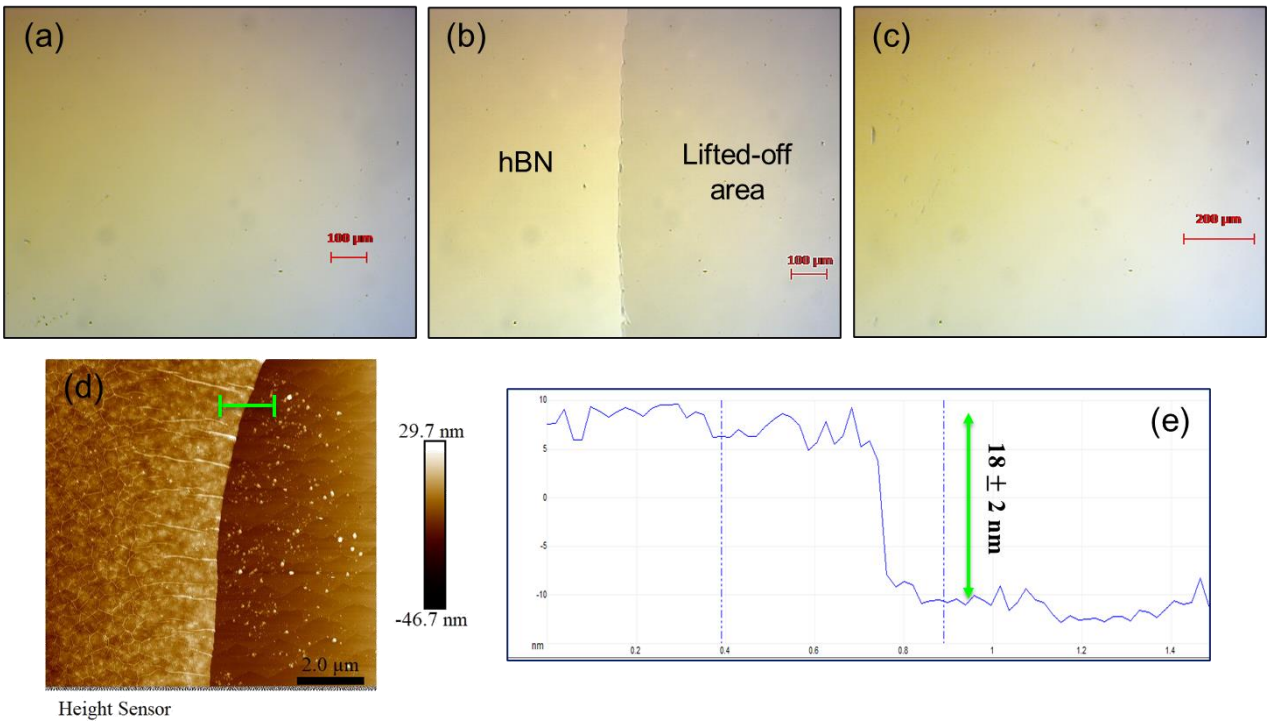

Fig. 3: (a-c) Optical microscope of 20 nm h-BN grown on a-, c-, m-plane sapphire and AFM image (d-e) of 20 nm h-BN grown on c-plane sapphire after lift-off.

We first conclude that there is an impact of the sapphire substrate orientation on the morphology, structural properties and the mechanical lift-off of h-BN layers. Under our growth temperature (~1280°C), h-BN exhibits a preferred orientation which is *c*-axis with slight misorientation on *m*-plane sapphire. In addition, mechanical lift-off and spontaneous delamination of this material can be prevented when grown on *a*- and *m*-plane sapphire, resulting in mechanically inseparable robust h-BN layers. This investigation of the impact of different orientation sapphire substrates on h-BN layers provides deeper insight and support for a better understanding of the growth mechanism for vdW epitaxy of GaN/AlGaN on h-BN/*a*-, *c*-, and *m*-plane sapphire, which is presented in the following.

The indirect influence of different orientation of sapphire substrates through hBN on vdW epitaxy of GaN was studied by growing 500 nm GaN/300 nm AlGaN (14%Al) on 1.5 nm h-BN on *a*-, *c*-, and *m*-plane sapphire. The surface morphology of these samples is shown in figure 4. The surface morphology of GaN/AlGaN/h-BN layers grown on *a*- and *c*-plane sapphire were smooth with the presence of V-pits, more markedly for the sample grown on *a*-plane sapphire, indicating varying degrees of the GaN layer coalescence (figures 4a-b). On contrary, 3D GaN

morphology is present on *m*-plane sapphire as shown in figure 4c. The surface exhibits the terraced structure, indicating that the GaN is not highly oriented along *c*-axis. This can be related to the above results of the misoriented hBN grown on *m*-plane sapphire, which can induce excess of misorientation spread. These results indicate that the different sapphire orientation affects the quality of the h-BN layer (discussed above), and this impacts the morphology of the GaN layer grown on ultra-thin h-BN layer. Further characterizations which were performed to validate this and will be discussed below.

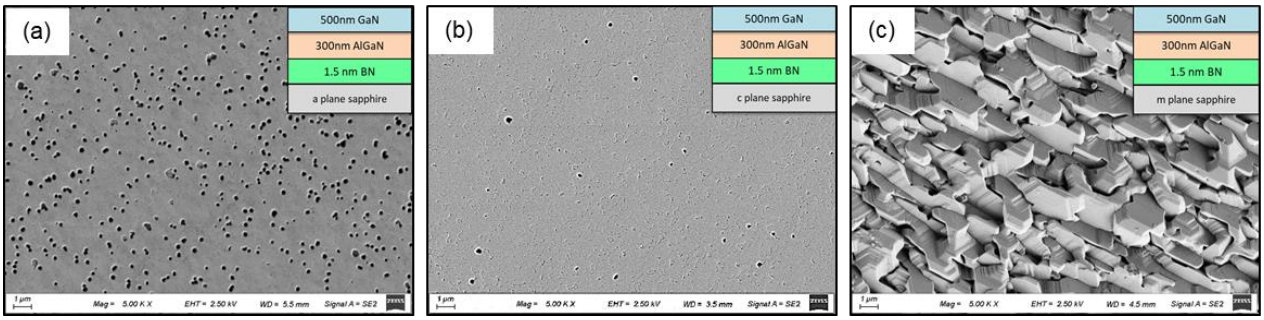

Fig. 4. SEM images of GaN/AlGaN (14%Al)/1.5nm h-BN on: (a) a-plane sapphire, (b) c-plane sapphire and (c) m-plane sapphire.

Additionally, HR-XRD measurements were made on the GaN films grown on h-BN layers on different oriented sapphire substrates. The 2θ-ω scan, in the 20°-80° measurement range were performed for the three samples as shown in figure 5a. For GaN/AlGaN/h-BN grown on *a*- and *c*-plane sapphire substrates, two diffraction peaks were clearly identified at 34.55° and 34.79°, which correspond to the (002) reflection of *ω*-GaN and buffer layer *ω*-AlGaN (14% Al), respectively. No other diffraction peak related to GaN was observed by HR-XRD scans, suggesting a good *c*-axis alignment of the GaN/AlGaN/h-BN grown on *a*- and *c*-plane sapphire substrates. On the other hand, the 2θ-ω scan of GaN/AlGaN/h-BN grown on *m*-plane sapphire exhibits several low intensity diffraction peaks at 34.7°, 46.3° and 63.2°. The closest crystallographic planes corresponding to these values are (002) GaN, (102) GaN and (103) GaN, respectively [35,36]. The intensity of the (002) GaN peak increases from *m*-, *a*- to *c*-plane sapphire substrates, which is in accordance with the (002) h-BN peak intensities reported in the previous section (figure 2a). Figure 5b shows the rocking curves of the GaN (002) peak for the three samples. We determine the FWHM values to be 0.39°, 0.29°, and 1.18° for *a*-, *c*-, and *m*-plane sapphire respectively. The (002) diffraction peak is affected by screw dislocations, and the dislocation density is estimated to

be 4E+09/cm^2, 2.2E+09/cm^2, and 5.1E+10/cm^2 for GaN/AlGaN/BN on *a*-, *c*-, and *m*-plane sapphire respectively. The lower dislocation density of GaN/AlGaN/BN on *c*-plane supports for the observation in SEM images (figure 4). Furthermore, the φ scan for a (102) plane of the three samples were also performed (see figure S3 - Supplementary).

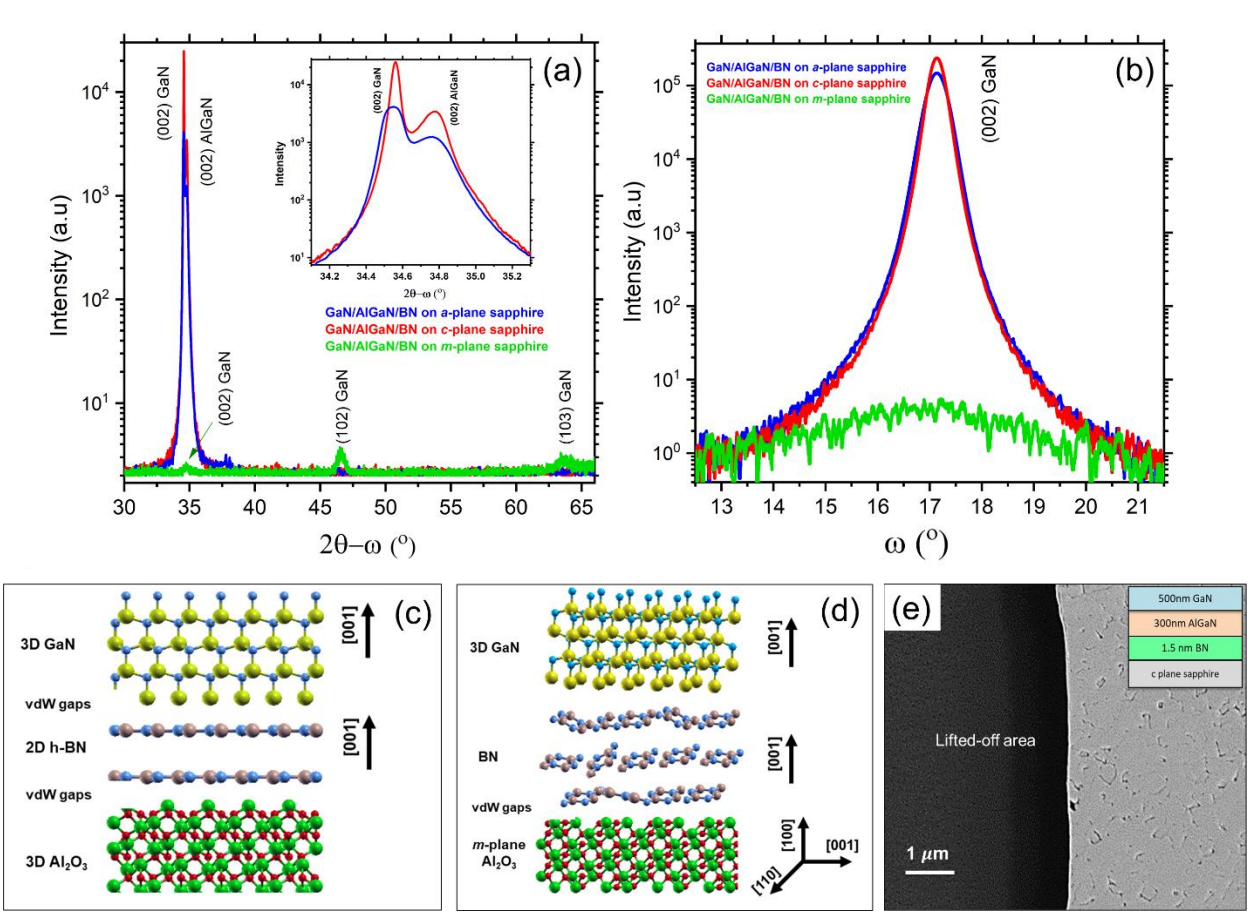

Fig. 5. (a) 2θ-ω scan and (b) (002) rocking curve of GaN/AlGaN/1.5 nm h-BN on a-, c- and m-plane sapphire; (c-d) schematic of preferred orientation of GaN/AlGaN/BN grown on different sapphire orientation (e) SEM image of GaN/ AlGaN/1.5 nm h-BN on c-plane sapphire after lift-off.

These results of both 2θ-ω scan and (002) rocking curve suggest that the preferred orientation of GaN is *c*-axis, effected directly from structural property of h-BN layers as seen in figure 5c, showing the schematic of preferred orientation of GaN/AlGaN/BN grown on oriented sapphire. The observation of (102) and (103) diffraction peaks and the high value of screw dislocation density for GaN/AlGaN/h-BN grown on *m*-plane sapphire provides enough evidence indicating the misorientation of the GaN film, which is caused due to the impact of BN layers grown on *m*-plane sapphire (figure 5d).

Mechanical lift-off was also performed for the three GaN/AlGaN/h-BN on *a*-, *c*-, and *m*-plane sapphire samples. Similar to the 20 nm h-BN, only GaN/AlGaN/1.5 nm h-BN grown on *c*-plane sapphire is able to lift-off, as seen in figure 5e, displaying the SEM image of this sample after lift-off. On the other hand, the GaN/AlGaN/1.5 nm h-BN on *a*- and *m*-plane sapphire has a strong adhesion, and it was not possible to detach it. This effect agrees with the observation of 20 nm h-BN as presented above. The SEM, XRD and mechanically lift-off results of GaN/AlGaN/h-BN provide strong evidence for the direct influence of h-BN layers on III-Nitride morphology, lift-off possibility and growth orientation. Moreover, the observation of the 3D morphology of GaN/AlGaN/1.5 nm h-BN grown on *m*-plane sapphire, resulting from the disoriented h-BN/*m*-plane sapphire can be seen clearly. Subsequently, we can conclude that there is an indirect impact of sapphire substrates on III-Nitride vdW epitaxy growth based h-BN layers.

Finally, detailed structural analysis of the GaN/AlGaN/h-BN grown on different sapphire planes was performed by HAADF-STEM as shown in Figure 6a-c for dark field images. The directions of the TEM observation are <0110>, <1011>, and <0111> for *a*-, *c*-, and *m*-plane sapphire samples as displayed in figure 6a-c. From the contrast of the STEM images obtained for different growth materials, the GaN, AlGaN and h-BN layers are observed, distinguished by red lines in figure 6a-c. The thickness of the AlGaN and GaN layer was estimated to be approximately 300 and 500 nm, respectively. We also observe a thin continuous layer of h-BN represented by a thin, higher contrast area at the bottom of these figures. The threading dislocation density (TDD) is estimated to be around 5E+09/cm^2 for GaN/AlGaN/h-BN on *a*- and *c*-plane sapphire. The slight difference in TDD of GaN compared to calculation based on FWHM (002) rocking curve can be attributed to the limitation of grid size in TEM measurements. These dislocations may originate from the AlGaN layer and can be explained by the growth mechanism of 3D layers on 2D crystals. Indeed, since the III-Nitride structure is grown on h-BN surface with no dangling bonds, these threading dislocations mostly originate from the formation of grain boundaries during the nucleation of AlGaN layer on h-BN [37]. For GaN/AlGaN/h-BN grown on *m*-plane, the cross-section STEM image is completely different when compared to *a*- and *c*-plane, where a terraced structure has been observed, in agreement with the SEM image.

Further, figures 6d-f show zoomed-in images of both the Al_2O_3/h-BN and h-BN/AlGaN interfaces. The TEM images exhibit a crystalline structure of 2-3 layers h-BN with the lattice

oriented along the *c*-axis for *a*- and *c*-plane sapphire. The interlayer distance of the h-BN layers is calculated to be 0.359 ± 0.003 nm for *a*- and *c*-plane sapphire. In case of *m*-plane sapphire, the h-BN sheets are not sufficiently well oriented, with respect to the substrate, leading to the lack of visibility of BN structure. In addition, we observed an un-intentionally grown AlN layer at the sapphire/h-BN interface in all the three samples, which may be due to nitridation. It is confirmed from the obtained AlN peak in GIXRD measurement of h-BN on *a*-plane sapphire (mentioned above). The orientation of the AlN layers underneath BN layer is systematically *c*-axis for *a*- and *c*-plane sapphire, while for *m*-plane sapphire AlN seems amorphous (or polycrystalline). A similar observation has been previously reported [33] with the assumption that different growth temperature can affect the structural quality of AlN layer at sapphire/h-BN interface. However, we believe that apart from growth temperature, the structural quality of this AlN layer can also depend on the orientation of sapphire substrates, which will need further study to confirm.

To evaluate an orientation relationship existing between the GaN/AlGaN layers and h-BN as well as different oriented sapphire substrates, we have examined selected area electron diffraction (SAED) pattern for oriented sapphire substrates (see supplementary-section 4) and for the AlGaN layer of the three samples as shown in figure 6 g-i. A well-ordered SAED pattern with single orientation spots can be seen for the samples grown on *a*- and *c*-plane sapphire substrates (figure 6g&h), indicating good crystalline quality of the AlGaN layer. The growth axis for the both AlGaN layers is [001], independent of the sapphire substrate orientation, but in the same growth orientation with h-BN layers. For the sample grown on *m*-plane sapphire, the SAED pattern consists of split spots, indicating a misorientation of the AlGaN crystal (figure 6i). From these results, we can conclude that the AlGaN (or GaN) layer is *c*-plane oriented and is strongly impacted by the orientation of h-BN buffer layer.

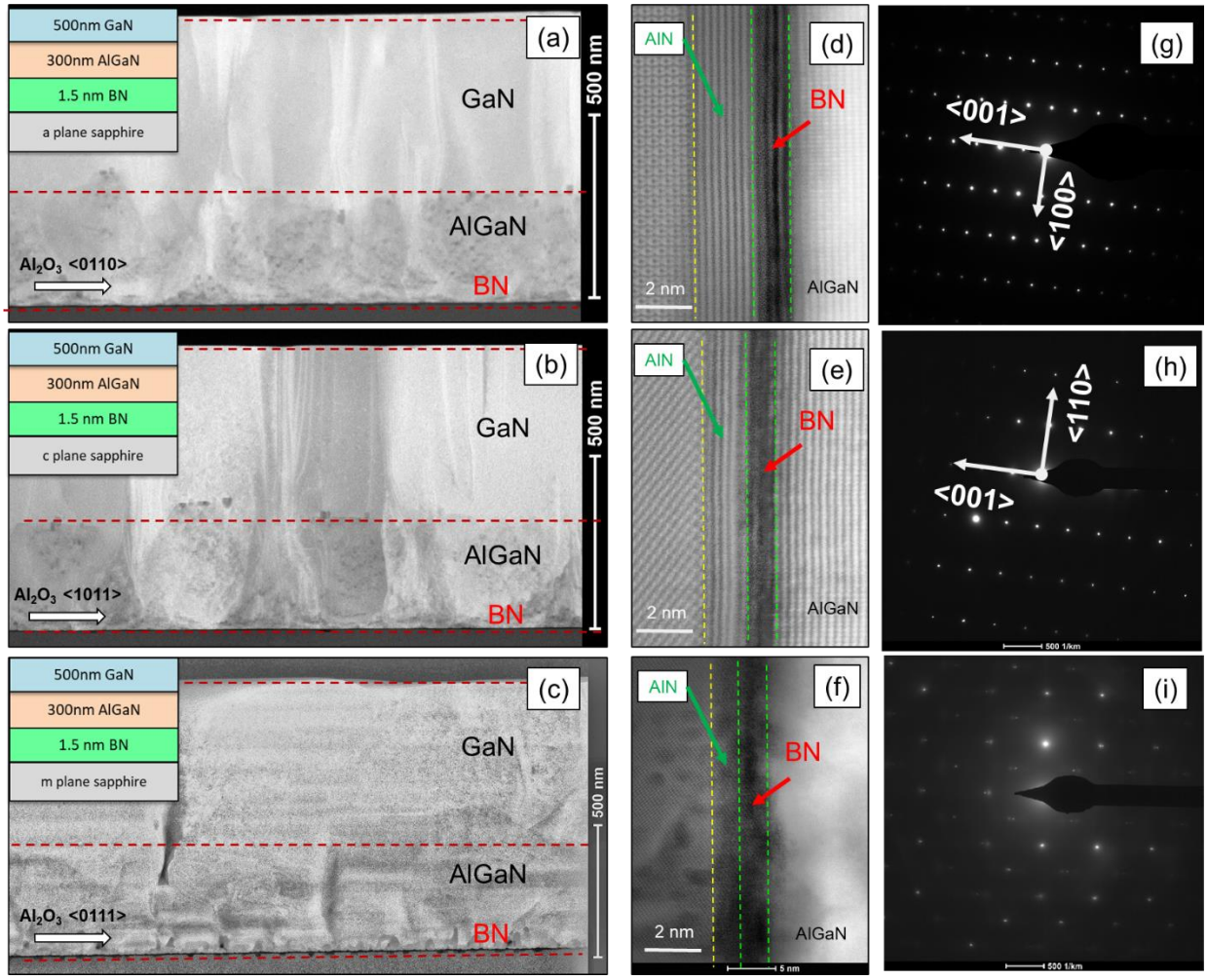

Fig. 6. (a-f) HAADF-STEM images of GaN/AlGaN/1.5 nm h-BN on a-, c- and m-plane sapphire; (g-i) Selected area electron diffraction (SAED) patterns was obtained from AlGaN layers of the three samples.

Conclusions

In summary, we have studied the effect of differently oriented sapphire substrate on 2D h-BN layer and on vdW epitaxy of 3D GaN/AlGaN on 2D h-BN materials. We found that there is an impact of sapphire substrates with different orientation on the morphology and structural properties of h-BN layer. Under certain growth temperature, h-BN can align itself to its preferred axis *c*-axis with a slight misorientation on *m*-plane sapphire. In addition, mechanical lift-off and spontaneous delamination of this material can be prevented when grow on *a*- and *m*-plane sapphire, resulting in mechanically inseparable robust h-BN layers. Further, vdW epitaxy of GaN/AlGaN exhibits strong dependence on h-BN layers from morphology to crystalline orientation. These results bring deeper understanding of vdW epitaxy combined with the orientation of sapphire

substrates, giving more potential approach of using h-BN or III-Nitride materials in opto-electronic devices such as LEDs, high power electronics and detectors.

Supporting information

The Supporting Information is available free of charge.

(i) Estimation of the growth rate of h-BN; (ii) Phi scan of h-BN/c-plane sapphire; (iii) Phi scan of GaN/AlGaN/BN on *a*-, *c*-, and *m*-plane sapphire; (iv) TEM image of GaN/AlGaN/BN and SAED pattern of the *a*-, *c*-, and *m*-plane sapphire

Acknowledgement

This study was partially funded by the French National Research Agency (ANR) under the GANEX Laboratory of Excellence (Labex) project and the Grand EST Region in France. It has been also partly supported by the French Renatech network and the ANR "Investissement d'Avenir" program (TEMPOS project no. ANR-10-EQPX-50).

Data availability

The data that support the findings of this study are available from the corresponding author upon reasonable request.

Notes:

The authors declare no conflict of interest.

References:

(1) Koma, A.; Sunouchi, K.; Miyajima, T. Fabrication and Characterization of Heterostructures with Subnanometer Thickness. *Microelectronic Engineering* **1984**, *2* (1), 129–136. https://doi.org/10.1016/0167-9317(84)90057-1.

(2) Chen, Q.; Yin, Y.; Ren, F.; Liang, M.; Yi, X.; Liu, Z. Van Der Waals Epitaxy of III-Nitrides and Its Applications. *Materials (Basel)* **2020**, *13* (17). https://doi.org/10.3390/ma13173835.

(3) Alaskar, Y.; Arafin, S.; Wickramaratne, D.; Zurbuchen, M. A.; He, L.; McKay, J.; Lin, Q.; Goorsky, M. S.; Lake, R. K.; Wang, K. L. Towards van Der Waals Epitaxial Growth of GaAs on Si Using a Graphene Buffer Layer. *Adv. Funct. Mater.* **2014**, *24* (42), 6629–6638. https://doi.org/10.1002/adfm.201400960.

(4) Koma, A. Van Der Waals Epitaxy for Highly Lattice-Mismatched Systems. *Journal of Crystal Growth* **1999**, *201–202*, 236–241. https://doi.org/10.1016/S0022-0248(98)01329-3.

(5) Liang, D.; Wei, T.; Wang, J.; Li, J. Quasi van Der Waals Epitaxy Nitride Materials and Devices on Two Dimension Materials. *Nano Energy* **2020**, *69*, 104463. https://doi.org/10.1016/j.nanoen.2020.104463.

(6) Li, Y.; Zhao, Y.; Wei, T.; Liu, Z.; Duan, R.; Wang, Y.; Zhang, X.; Wu, Q.; Yan, J.; Yi, X.; Yuan, G.; Wang, J.; Li, J. Van Der Waals Epitaxy of GaN-Based Light-Emitting Diodes on Wet-Transferred Multilayer Graphene Film. *Jpn. J. Appl. Phys.* **2017**, *56* (8), 085506. https://doi.org/10.7567/JJAP.56.085506.
(7) Zhou, H.; Xu, Y.; Chen, X.; Liu, Y.; Cao, B.; Yin, W.-J.; Wang, C.; Xu, K. Direct van Der Waals Epitaxy of Stress-Free GaN Films on PECVD Grown Graphene. *Journal of Alloys and Compounds* **2020**, *844*, 155870. https://doi.org/10.1016/j.jallcom.2020.155870.
(8) Chang, H.; Chen, Z.; Liu, B.; Yang, S.; Liang, D.; Dou, Z.; Zhang, Y.; Yan, J.; Liu, Z.; Zhang, Z.; Wang, J.; Li, J.; Liu, Z.; Gao, P.; Wei, T. Quasi-2D Growth of Aluminum Nitride Film on Graphene for Boosting Deep Ultraviolet Light-Emitting Diodes. *Advanced Science* **2020**, *7* (15), 2001272. https://doi.org/10.1002/advs.202001272.
(9) Kobayashi, Y.; Kumakura, K.; Akasaka, T.; Makimoto, T. Layered Boron Nitride as a Release Layer for Mechanical Transfer of GaN-Based Devices. *Nature* **2012**, *484* (7393), 223–227. https://doi.org/10.1038/nature10970.
(10) Ayari, T.; Sundaram, S.; Li, X.; El Gmili, Y.; Voss, P. L.; Salvestrini, J. P.; Ougazzaden, A. Wafer-Scale Controlled Exfoliation of Metal Organic Vapor Phase Epitaxy Grown InGaN/GaN Multi Quantum Well Structures Using Low-Tack Two-Dimensional Layered h-BN. *Applied Physics Letters* **2016**, *108* (17), 171106. https://doi.org/10.1063/1.4948260.
(11) Inoue, S.; Okamoto, K.; Matsuki, N.; Kim, T.-W.; Fujioka, H. Epitaxial Growth of GaN on Copper Substrates. *Appl. Phys. Lett.* **2006**, *88* (26), 261910. https://doi.org/10.1063/1.2213178.
(12) Ramesh, C.; Tyagi, P.; Bera, S.; Gautam, S.; Subhedar, K. M.; Senthil Kumar, M.; Kushvaha, S. S. Structural and Optical Properties of GaN Film on Copper and Graphene/Copper Metal Foils Grown by Laser Molecular Beam Epitaxy. *J Nanosci Nanotechnol* **2020**, *20* (6), 3929–3934. https://doi.org/10.1166/jnn.2020.17536.
(13) Cho, H.; Park, S.; Won, D.-I.; Kang, S. O.; Pyo, S.-S.; Kim, D.-I.; Kim, S. M.; Kim, H. C.; Kim, M. J. Growth Kinetics of White Graphene (h-BN) on a Planarised Ni Foil Surface. *Sci Rep* **2015**, *5*, 11985. https://doi.org/10.1038/srep11985.
(14) Yu, Y.; Wang, T.; Chen, X.; Zhang, L.; Wang, Y.; Niu, Y.; Yu, J.; Ma, H.; Li, X.; Liu, F.; Deng, G.; Shi, Z.; Zhang, B.; Wang, X.; Zhang, Y. Demonstration of Epitaxial Growth of Strain-Relaxed GaN Films on Graphene/SiC Substrates for Long Wavelength Light-Emitting Diodes. *Light Sci Appl* **2021**, *10* (1), 117. https://doi.org/10.1038/s41377-021-00560-3.
(15) Nepal, N.; Wheeler, V. D.; Anderson, T. J.; Kub, F. J.; Mastro, M. A.; Myers-Ward, R. L.; Qadri, S. B.; Freitas, J. A.; Hernandez, S. C.; Nyakiti, L. O.; Walton, S. G.; Gaskill, K.; Charles R Eddy, J. Epitaxial Growth of III–Nitride/Graphene Heterostructures for Electronic Devices. *Appl. Phys. Express* **2013**, *6* (6), 061003. https://doi.org/10.7567/APEX.6.061003.
(16) Bruni, F. Crystal Growth of Sapphire for Substrates for High-Brightness, Light Emitting Diodes. *Crystal Research and Technology* **2014**, *50*. https://doi.org/10.1002/crat.201400230.
(17) Ryou, J.-H.; Lee, W. 3 - GaN on Sapphire Substrates for Visible Light-Emitting Diodes. In *Nitride Semiconductor Light-Emitting Diodes (LEDs) (Second Edition)*; Huang, J., Kuo, H.-C., Shen, S.-C., Eds.; Woodhead Publishing Series in Electronic and Optical Materials; Woodhead Publishing, 2018; pp 43–78. https://doi.org/10.1016/B978-0-08-101942-9.00003-4.
(18) Wang, W.; Yang, W.; Wang, H.; Zhu, Y.; Yang, M.; Gao, J.; Li, G. A Comparative Study on the Properties of C-Plane and a-Plane GaN Epitaxial Films Grown on Sapphire Substrates by Pulsed Laser Deposition. *Vacuum* **2016**, *C* (128), 158–165. https://doi.org/10.1016/j.vacuum.2016.03.032.

(19) Wernicke, T.; Netzel, C.; Weyers, M.; Kneissl, M. Semipolar GaN Grown on M-plane Sapphire Using MOVPE. *physica status solidi (c)* **2008**, *5*, 1815–1817. https://doi.org/10.1002/pssc.200778670.
(20) Armitage, R.; Hirayama, H. M-Plane GaN Grown on m-Sapphire by Metalorganic Vapor Phase Epitaxy. *Appl. Phys. Lett.* **2008**, *92* (9), 092121. https://doi.org/10.1063/1.2894509.
(21) Ambacher, O.; Dimitrov, R.; Stutzmann, M.; Foutz, B. E.; Murphy, M. J.; Smart, J. A.; Shealy, J. R.; Weimann, N. G.; Chu, K.; Chumbes, M.; Green, B.; Sierakowski, A. J.; Schaff, W. J.; Eastman, L. F. Role of Spontaneous and Piezoelectric Polarization Induced Effects in Group-III Nitride Based Heterostructures and Devices. *physica status solidi (b)* **1999**, *216* (1), 381–389. https://doi.org/10.1002/(SICI)1521-3951(199911)216:1<381::AID-PSSB381>3.0.CO;2-O.
(22) Li, X.; Sundaram, S.; El Gmili, Y.; Ayari, T.; Puybaret, R.; Patriarche, G.; Voss, P. L.; Salvestrini, J. P.; Ougazzaden, A. Large-Area Two-Dimensional Layered Hexagonal Boron Nitride Grown on Sapphire by Metalorganic Vapor Phase Epitaxy. *Crystal Growth & Design* **2016**, *16* (6), 3409–3415. https://doi.org/10.1021/acs.cgd.6b00398.
(23) Chugh, D.; Wong-Leung, J.; Li, L.; Lysevych, M.; Tan, H. H.; Jagadish, C. Flow Modulation Epitaxy of Hexagonal Boron Nitride. *2D Materials* **2018**, *5* (4), 045018. https://doi.org/10.1088/2053-1583/aad5aa.
(24) Sundaram, S.; Li, X.; Alam, S.; Halfaya, Y.; Patriarche, G.; Ougazzaden, A. Wafer-Scale MOVPE Growth and Characterization of Highly Ordered h-BN on Patterned Sapphire Substrates. *Journal of Crystal Growth* **2019**, *509*, 40–43. https://doi.org/10.1016/j.jcrysgro.2018.12.016.
(25) Saha, S.; Rice, A.; Ghosh, A.; Hasan, S. M. N.; You, W.; Ma, T.; Hunter, A.; Bissell, L. J.; Bedford, R.; Crawford, M.; Arafin, S. Comprehensive Characterization and Analysis of Hexagonal Boron Nitride on Sapphire. *AIP Advances* **2021**, *11* (5), 055008. https://doi.org/10.1063/5.0048578.
(26) Leszczynski, M.; Suski, T.; Teisseyre, H.; Perlin, P.; Grzegory, I.; Jun, J.; Porowski, S.; Moustakas, T. D. Thermal Expansion of Gallium Nitride. *Journal of Applied Physics* **1994**, *76* (8), 4909–4911. https://doi.org/10.1063/1.357273.
(27) Miyagawa, R.; Wu, J.; Miyake, H.; Hiramatsu, K. Growth of High Quality C-Plane AlN on a-Plane Sapphire. *MRS Proc.* **2009**, *1202*, 1202-I05-02. https://doi.org/10.1557/PROC-1202-I05-02.
(28) Shigeya. N, 2021 GaN Remote-epitaxy on Graphene/r-plane Sapphire Substrates, *Epitaxy on 2D materials for layer release and their application conference*, https://weikonglab.wixsite.com/2021.
(29) Körber, C.; Suffner, J.; Klein, A. Surface Energy Controlled Preferential Orientation of Thin Films. *Journal of Physics D: Applied Physics* **2010**, *43*, 055301. https://doi.org/10.1088/0022-3727/43/5/055301.
(30) Pu, Z.; Dillon, O. W.; Puelo, D. A.; Jawahir, I. S. 5 - Cryogenic Machining and Burnishing of Magnesium Alloys to Improve in Vivo Corrosion Resistance. In *Surface Modification of Magnesium and its Alloys for Biomedical Applications*; Narayanan, T. S. N. S., Park, I.-S., Lee, M.-H., Eds.; Woodhead Publishing Series in Biomaterials; Woodhead Publishing, 2015; pp 103–133. https://doi.org/10.1016/B978-1-78242-078-1.00005-0.
(31) Nosov, Yu. G.; Bakholdin, S. I.; Krymov, V. M. Faceting of Sapphire Crystals Grown from a Melt by the Stepanov Method. *Tech. Phys.* **2009**, *54* (2), 239–245. https://doi.org/10.1134/S1063784209020133.
(32) Bakholdin, S. I.; Maslov, V. N. Simulation of Surface Energies of Sapphire Crystals. *Phys. Solid State* **2015**, *57* (6), 1236–1243. https://doi.org/10.1134/S1063783415060037.

(33) Vuong, P.; Sundaram, S.; Mballo, A.; Patriarche, G.; Leone, S.; Benkhelifa, F.; Karrakchou, S.; Moudakir, T.; Gautier, S.; Voss, P.; Salvestrini, J.; Ougazzaden, A. Control of the Mechanical Adhesion of III−V Materials Grown on Layered H-BN. *ACS Applied Materials & Interfaces* **2020**, *12*, 55460. https://doi.org/10.1021/acsami.0c16850.
(34) Sundaram, S.; Vuong, P.; Mballo, A.; Ayari, T.; Karrakchou, S.; Patriarche, G.; Voss, P.; Salvestrini, J.; Ougazzaden, A. MOVPE of GaN-Based Mixed Dimensional Heterostructures on Wafer-Scale Layered 2D Hexagonal Boron Nitride—A Key Enabler of III-Nitride Flexible Optoelectronics. *APL Materials* **2021**, *9*, 061101. https://doi.org/10.1063/5.0049306.
(35) Pang, H.; Liu, L.; Ouyang, S.; Xu, H.; li, Y.; Wang, D. Structure, Optical Properties, and Photocatalytic Activity towards H2 Generation and CO2 Reduction of GaN Nanowires via Vapor-Liquid-Solid Process. *International Journal of Photoenergy* **2014**, *2014*. https://doi.org/10.1155/2014/894396.
(36) Keyan, B.; Liang, S.; Xiaodi, L.; Changzhong, C.; Wutao, M.; Lingling, Z.; Jie, C. Synthesis of GaN Nanorods by a Solid-State Reaction. *Journal of Nanomaterials* **2010**, *2010*. https://doi.org/10.1155/2010/271051.
(37) Karrakchou, S.; Sundaram, S.; Ayari, T.; Mballo, A.; Vuong, P.; Srivastava, A.; Gujrati, R.; Ali, A.; Patriarche, G.; Thierry, L.; Gautier, S.; Moudakir, T.; Voss, P.; Salvestrini, J.; Ougazzaden, A. Effectiveness of Selective Area Growth Using van Der Waals H-BN Layer for Crack-Free Transfer of Large-Size III-N Devices onto Arbitrary Substrates. *Scientific Reports* **2020**, *10*. https://doi.org/10.1038/s41598-020-77681-z.